

**Crawfish Derived Nitrogen Doped Carbon as Electrode Materials for Sodium Ion
Batteries**

A Thesis

Submitted on the Twelfth Day of May 2021

To the Department of Physics and Engineering Physics

Of Tulane University

In Partial Fulfillment of the Requirements

For the Degree of Master of Science

In Materials Science and Engineering

By

Hudson McKinley

Hudson McKinley

Approved by:

Michael Naguib

Digitally signed by Michael Naguib
DN: cn=Michael Naguib, o, ou,
email=naguib@tulane.edu, c=US
Date: 2021.05.13 15:45:07 -05'00'

Michael Naguib, Ph.D.

Douglas Chrisey

Douglas Chrisey, Ph.D.

Matthew Escarra

Matthew Escarra, Ph.D.

ABSTRACT

Various organic precursors can be utilized to form activated carbons by using an assortment of chemical and physical activation processes.⁵ Picking certain biomaterials, ideally biomass byproducts, can allow advantageous performance by taking advantage of the naturally occurring structure and chemical makeup of the material. The goal of the work in this thesis is to use crawfish shell waste as a low-cost energy storage material while maintaining respectable capacitance and cyclability. The exoskeleton of crawfish contains 23.5% chitin, which is a biopolymer extremely rich in both carbon and nitrogen,⁴ and has a porous structure; theoretically making it an ideal electrochemical storage material. For treatment, the shells are rinsed using HCl, NaOH, and KOH to remove unwanted compounds, increase nitrogen content, and serve as an activation catalyst for the material. Electrodes were assembled on both C-coated Cu and low-cost Al foils, and tested for anode rate capability, cyclability, and cyclic voltammetry. The material was found to achieve a gravimetric capacity in excess of 175mAh/g on Cu, and around 150mAh/g on Al at low rates of 20mA/g and 50mA/g respectively, and maintain a capacity around 100mAh/g at a high rate of 200mA/g, but with decreasing performance over long-term cycling.

ACKNOWLEDGEMENTS

First and foremost I would like to thank Michael Naguib, Ph.D for allowing me to perform both my undergraduate and graduate research as part of his blossoming and diverse group, and for all of the knowledge and guidance he has bestowed upon me throughout my time spent in his lab. I would also like to thank Kaitlyn Prenger and Kun Liang for their guidance in cell assembly and testing. Additionally, thanks to Shae Jolly who aided in the EDS analysis and operation of the vacuum furnace that were used in this experiment. Special thanks to Eliza LaRue for extensive help with the de-shelling of the crawfish. Lastly, thank you to all other members of the research group for helping in many small ways throughout the time this research was being conducted.

TABLE OF CONTENTS

LIST OF FIGURES	5
1. INTRODUCTION.....	8
2. BACKGROUND.....	9
2.1 Importance	9
2.2 Biofuel Material Properties	12
2.3 Applied Processes	14
3. METHODS	17
3.1 Shell Biorefinery	17
3.2 Electrode Preparation.....	20
3.3 Cell Assembly	22
4. RESULTS	27
5.1 Shell Biorefinery	27
5.2 Electrochemistry of Supercapacitors	35
5. DISCUSSION	38
6. CONCLUSION	41
7. REFERENCES	42

LIST OF FIGURES

Figure 2.1	11
Calculated cell material costs for the reference LiMn_2O_4 (LMO)–sG battery and a theoretical LMO–sG battery in which the copper foil is replaced with aluminum foil and lithium is replaced with sodium. The diagonal lines indicate that there is a change in the cost of a component between the two systems. ¹⁶	
Figure 2.2	13
Chitosan is converted to activated carbon with a very porous microtexture. ¹⁰ The surface capacitance of carbon is greater when nitrogen is added due to the desirable stable properties of nitrogen. ¹⁰	
Figure 3.1	17
The cooking pot for the live crawfish.	
Figure 3.2	18
The reflux setup for the KOH step of the procedure	
Figure 3.3	19
The vacuum furnace for the carbonization step	
Figure 3.4	20
Hitachi S-3400 SEM used for EDS measurements	
Figure 3.5	21
The SPEX mill used to prepare the carbonized material	
Figure 3.6	22
Prepared electrodes using Al current collectors and Drop Casting	
Figure 3.7	23
(From Left to Right) The positive battery lid, an electrode, the glass fiber separator, a piece of raw sodium, the stainless-steel current collector, a washer spring, and the negative terminal of the coin cell. Also pictured is a bottle of the NaFP6 electrolyte.	

Figure 3.8	23
The cell press used to crimp the coin cells	
Figure 3.9	24
Assembled CR2032 Coin Cell	
Figure 3.10	25
The LAHNE cyclor channels with connections running to the environmental chamber adjacent	
Figure 3.11	25
The Biologic VMP3 Potentiostat used for CV measurements	
Figure 3.12	26
The inside of the environmental testing chamber	
Figure 4.1	28
Results from the BET analysis	
Figure 4.2	29
(A) Crawfish shells after the boiling and drying process. (B) EDS produced table showing the elemental weight and atomic percent of the boiled crawfish.	
Figure 4.3	29
(A) Crawfish shells after being soaked in HCL. (B) EDS produced table showing the elemental weight and atomic percents of the HCL soaked crawfish after washing.	
Figure 4.4	30
(A) Deproteinized chitin dominant crawfish after being soaked in NaOH. (B) EDS produced table showing the elemental weight and atomic percents of the NaOH soaked crawfish after washing.	
Figure 4.5	30
(A) Deacetylied chitosan dominant crawfish shells after being refluxed in KOH. (B) EDS produced table showing the elemental weight and atomic percents of the KOH refluxed crawfish.	

Figure 4.6	31
(A) Carbonized biomass. (B) EDS produced table showing the elemental weight and atomic percents of the carbonized crawfish.	
Figure 4.7	31
EDS produced table showing the element weight and atomic percents of the carbonized and washed crawfish.	
Figure 4.8	32
High magnification SEM image showing the mesoporous structure of the activated carbon.	
Figure 4.9	32
Long term cycling at 20mA on electrode with active mass of 1.26mg and 200mA on electrode with an active mass of 1.44mg	
Figure 4.10	33
Rate Capability performed at 50mA, 100mA, 200mA, 500mA, 1000mA, and 50mA respectively on C-Cu substrate electrode with active mass loading of 1.4mg.	
Figure 4.11	33
Voltage profile of the 1.26mg loaded cell from figure 8 for selected cycles.	
Figure 4.12	34
CV performed on a cell with loading of 1.3mg on Carbon coated Copper substrate.	
Figure 4.13	34
Rate Capability performed at 50mA, 100mA, 200mA, 500mA, 1000mA, and 50mA respectively on Al substrate electrode with active mass loading of 1.4mg.	
Figure 4.14	35
Cycling performance of graphite reference Cells with loading of 1.34mg at 50mA and 1.15mg at 100mA	

1. INTRODUCTION

Every year, an estimated 6 to 8 million tons of shell waste is created, almost none of which is repurposed.¹ However, the exoskeleton of crawfish contains 23.5% chitin, which is a biopolymer extremely rich in both carbon and nitrogen.² Through demineralization and deproteinization, chitin is extracted from the crawfish shells. Soaking this chitin in a basic solution at high temperatures removes an acetyl group to produce chitosan,² which is a linear polysaccharide with a porous structure.

Carbonization, heating at a high temperature for an extended period of time, can be performed to any biomass to break down compounds and yield carbon. To prepare material that will be activated when carbonized, chitosan is refluxed in a strong potassium hydroxide (KOH) solution. This will induce morphologic changes and create mesopores in the resulting carbon. Characterization is performed by analysis using energy dispersion spectroscopy (EDS), scanning electron microscopy (SEM), rate capability testing (RC), and cyclic voltammetry (CV).

By utilizing the inherent properties of crawfish shells as three-dimensional anode material, the electronic layer ion electrosorption is accelerated while a nitrogen-doped mesoporous structure maximizes energy density. This novel energy material is applied to sodium ion batteries, which are low cost, have abundant natural availability, and provide increased charge and discharge rate performance compared to that of their lithium counterpart.³ The increased interstitial porous space within the crawfish derived activated hard carbon is beneficial in promoting movement and transfer of the large sodium ions. Ultimately, sourcing material from an environmentally friendly biomaterial improves energy storage while simultaneously reprocessing waste.

2. BACKGROUND

2.1 Importance

2.1.1 Energy Storage

One thing that people have been working on since the beginning of time is the ability to accumulate resources when they're abundant, for use when they are not. This ranges from agriculture compared to foraging, living by fresh water, and most prevalent today; energy storage. With the design of most energy generation techniques, they are available at high volumes over short periods of time. This is not ideal for general use purposes as all utilization is dependent on production. Energy storage allows all of the power generated to be stored for when it is needed. A common example of this would be solar power. It is extremely effective as a passive energy production method when sunlight is available, however energy is still necessary during all hours for activity to continue as usual. This is where an energy storage device is necessary to save that high output volume for later use. There are many different types of energy storage devices. Some are kinetic, such as flywheels which have an accelerating rotor that holds rotational energy for when it is needed later.¹⁴ It can be done with thermal retention such as seen in latent heat thermal (LHTES) that uses a phase change material to store energy by allowing it to revert back to its equilibrium phase later.¹⁵ However, the most common today, and focus of this investigation, is electrochemical energy storage.

2.1.2 Batteries

Batteries are known as secondary cells as they are electrically reversible and allow an electric input to cause a chemical reaction that can be reversed later to release the stored energy. The standard method for portable energy storage is the lithium ion (Li^+) battery. They serve as an electronic tool that provides charge and storage, and can serve many functions such as powering devices and other equipment. They work by introducing Li^+ into the electrodes, which results in delayed bulk solid diffusion-dependent redox reactions that provides energy.⁹ Although batteries produce a great amount of energy storage and density capabilities per unit mass, they charge slowly. Also, batteries are only applicable for low current in a long-term setting. There are many advantages to batteries such as their easy use and abundance, but disadvantages are also present. There are novel methods being researched that modify current batteries by integrating new energy storage and charge properties within the battery.⁹ These aim to improve the current energy storage landscape and continue its rapid growth as a field that has a large impact on people's day to day living.

2.1.3 Issues with the Li ion Battery

As mentioned in the introduction, a primary objective of this investigation is to produce a low-cost material for energy storage. Lithium batteries do not allow this due to its intrinsic scarcity and therefore high cost. While the theoretical storage limit of lithium is higher at 278 Wh/kg¹⁷, this doesn't tell the whole story. In modern lithium ion battery architecture, only 2.5% of the cell is composed of the charge carrier.¹⁶ The majority is the electrode materials, electrolyte, separators, and current collector.¹⁶ When considering that common anode materials such as graphite can accommodate sodium to the same level as

lithium, there is really only a 10% lower theoretical capacity.¹⁶ This is due to how the same amount of materials can be placed in the same amount of area, and the only difference is from their energy densities.

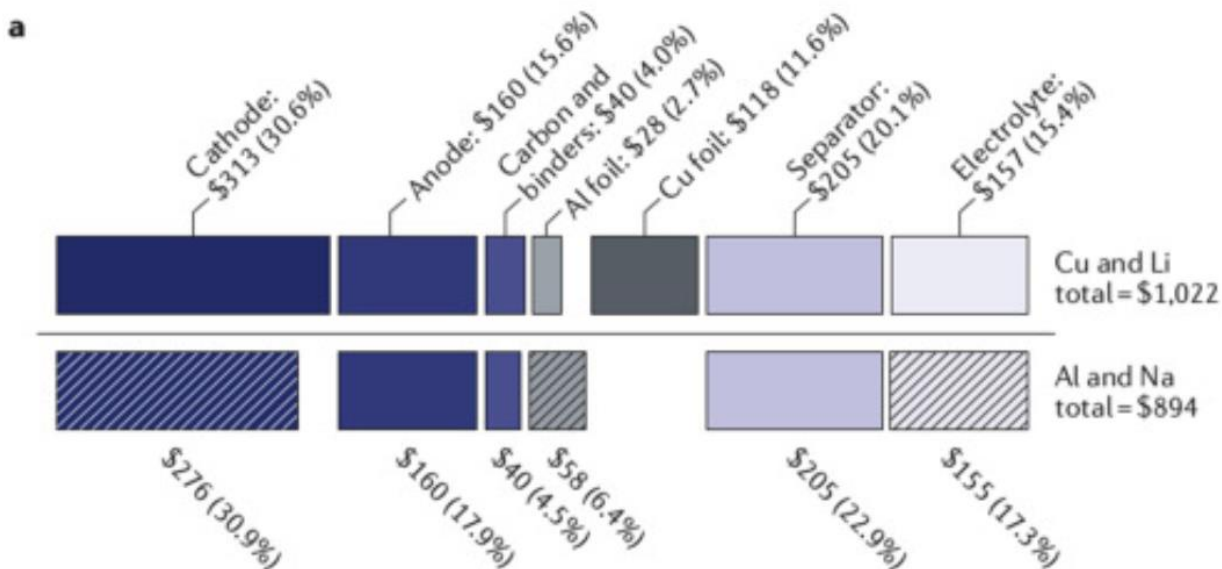


Figure 2.1: Calculated cell material costs for the reference LiMn_2O_4 (LMO)–Silicon-graphite battery and a theoretical LMO–Si-graphite battery in which the copper foil is replaced with aluminum foil and lithium is replaced with sodium. The diagonal lines indicate that there is a change in the cost of a component between the two systems.¹⁶

2.1.4 Advantages of the Na ion Battery

The natural resources for sodium are 1000x that of lithium.¹⁶ This not only lowers the potential long-term cost, but reduces impact of extraction as well. Additionally, this allows research on a whole new class of materials that are not ideal for Li ion systems, potentially opening the door for much better performance than thought possible due to lack of attention by the academic community over the past 50 years. Also, it is possible to replace the expensive and heavy Cu current collector with Al. This has a potential improvement of 2% in the theoretical max specific energy. Also, the Al doesn't alloy

with sodium, so it can be used as the current collector for both the anode and cathode sides; reducing cost by 8% and increasing the specific energy by 2% due to the fraction of weight when compared to Copper.¹⁶

2.2 Biofuel Material Properties

2.2.1 Conversion from Reactant to Product

In the introduction we stated that the biopolymer of interest within the shell is chitin, and a similar compound that is easily created from chitin; chitosan. When the degree of deacetylation of chitin is around 50%, it becomes soluble in aqueous acidic media and is called chitosan.¹¹ The solubility is due to the protonation of $-NH_2$ to the compound, which yields a polyelectrolyte¹¹. Overall, utilizing chitosan instead of chitin is advantageous due to the increased solubility of chitosan in aqueous solution and its unbound reactive amino group that is readily protonated and deprotonated.

2.2.2 Advantage of Chitosan

The percent of nitrogen in chitosan is 8.69% per mole, while it is only 6.88% per mole in chitin.⁶ This is a considerable increase and definitely worth the extra steps for the added nitrogen, as this should cause performance boost that neutralizes the poor conductivity, stability, and slow kinetics that hard carbon traditionally exhibits.¹⁸ Additionally, this nitrogen can induce a pseudo capacitance between the electrolyte and N-doped surface.¹⁸

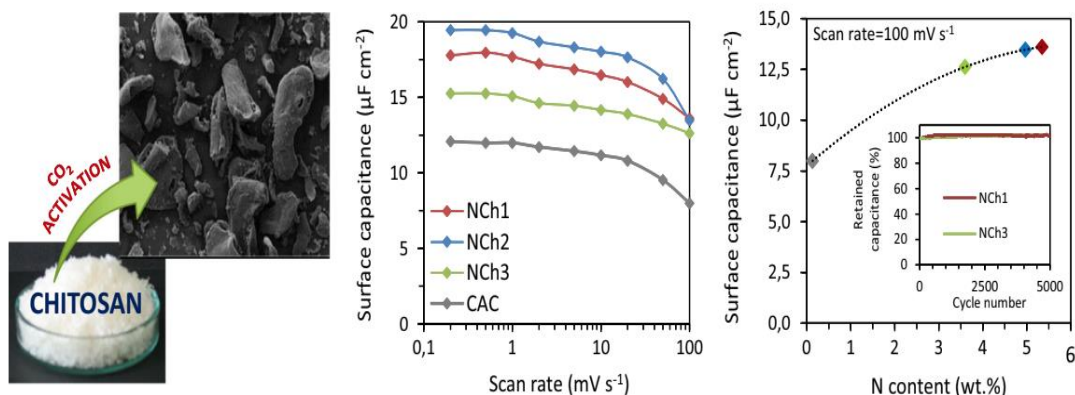


Figure 2.2: Chitosan is converted to activated carbon with a very porous microtexture.¹⁰ The surface capacitance of carbon is greater when nitrogen is added due to the desirable stable properties of nitrogen.¹⁰

2.2.3 Limitation of Chitosan

There is so much chitosan that is unused and wasted each year as processing byproduct. Chitosan is a natural biopolymer with physicochemical properties that have the potential of creating novel energy storage materials. This linear polysaccharide is polycationic, non-toxic, and biodegradable. However, chitosan solubility is low in basic and neutral solutions which means it has decreased efficiency in those conditions.¹⁰ Also, chitosan is derived from chitin through a deacetylation process. While this technique provides a wide range of practical uses, it may hinder the quality of chitosan. This is because the structural and functional characteristics of chitosan are determined by the quality of the chitin. Hence, chitosan's solubility, molar mass, and acetylation properties are directly dependent on the chitin extraction process, so any errors may result in a reduced chitosan chain crystalline structure.

2.2.4 Activated Carbon

Undergoing carbonization while saturated with an activating compound, chitosan is converted into activated carbon. This process consists of soaking the chitosan in acidic and basic solutions, refluxing with a strong base, heat treatment, and washing. There are many advantages of using activated carbon due to its acidic, thermal, and electrochemical stability. Also, it has a well-defined connected mesoporous microstructure with many small sized low-volume pores. Ultimately, this contributes to its high surface area and conductivity which increases the amount of potential chemical reactions that may occur both at the surface and in the bulk. There are several techniques to measure the electrochemical performance and characterize the pores on the lattice structure of activated carbon, such as Brunauer-Emmett-Teller (BET) surface analysis. Additionally, it's easy to process and store without the loss of its functions. Activated carbon is useful, specifically as an electrode material, due to its intrinsic properties that increase gravimetric capacitance.³ Lastly, there is a limited space capacity on the electrodes, so activated carbon's flexibility and adjustable dimensions make it very convenient to use.

2.3 Applied Processes

2.3.1 Techniques

To determine the effectiveness of activated carbon created from crawfish shells, several methods are applied to verify the calculated results. Energy dispersion spectroscopy and scanning electron microscopy display the composition and surface texture of the

activated carbon. The capacitive level after repeated charging and discharging is tested with cycling. There are two forms of this that are utilized in this investigation. Anode rate capability, which does 10-20 cycles per specific current to give an idea of the capabilities of the system; and long-term cycling, which shows the batteries performance over several hundred cycles and test its viability over long term use. The downside of this method is that it takes months to get a large dataset; while anode rate capability can be done in about a week.

2.3.2 Significance of the Statistics

This experiment is novel because it refines crawfish shells into a nitrogen-doped porous activated carbon that is assembled into a sodium ion battery. The electrochemical properties of this battery are compared to that of batteries constructed from inactivated carbon and other activated carbons. By graphing the results, the carbon acquired from crawfish shells should reveal improvements in capacitance and energy storage compared to that of other carbon products.

2.3.3 Future Implications

Improvements to the experiment and the next steps are to continue building these batteries, potentially supplementing them with supercapacitors so that the desirable properties of each respective material are prevalent.¹² Integrating the long-term storage of batteries with the quick charge and high conductivity of supercapacitors provides a new source of energy attained from bio-waste. Additionally, applying new methods that detect

surface morphology of activated carbon in order to gain further insight about unknown attributes of its structure and function.

3. METHODS

3.1 Shell Biorefinery

To begin, 30 lbs. of live crawfish (Louisiana Crawfish, Natchitoches, LA) was acquired as an accurate and fresh source of shell material. All the crawfish were put into one large cooking pot with boiling water over a large propane flame for 1 hour. This way the boiling method would be consistent throughout the entire sample. After straining out the water, the cephalothorax and abdomen of the crawfish were deshelled. Also, the meat in the pincer and walking legs were difficult to separate from the shell, so those parts were discarded.



Figure 3.1 :The cooking pot for the live crawfish.

The shells were dried overnight in an oven at 77 °C. The following day the dried shells are milled in a fruit blender until the particle size resembled sand. The crawfish shell powder that was yielded had a mass of 450 grams. The shells were soaked in 10% wt. HCl

at room temperature for 24 hours in order to remove the calcium carbonate.⁴ The acidic shells were rinsed with deionized water using vacuum filtration until a neutral pH was achieved. This removed any residual HCl and CaCO₃. The elemental weight composition and atomic percent of the shells after this step was processed and verified using energy dispersion spectroscopy (EDS) and pH measurements to make sure that the chlorine ions had been removed. Then, the crawfish shells were soaked in 9% wt. NaOH solution with a 1:1 weight ratio at 95 °C for 2 hours.⁴ The solution was heated in a mineral oil bath to ensure equal thermal distribution. The basic shells were rinsed with deionized water using vacuum filtration until a neutral pH was achieved, yielding shells that were primarily composed of chitin. The composition of the shells after this step was verified using EDS and pH measurements to make sure the sodium ions had been removed. The shells were refluxed at 75°C and stirred in 100 mL of 40% wt. KOH for 5 hours to yield C₆H₁₁NO₄ or chitosan sugar.⁴

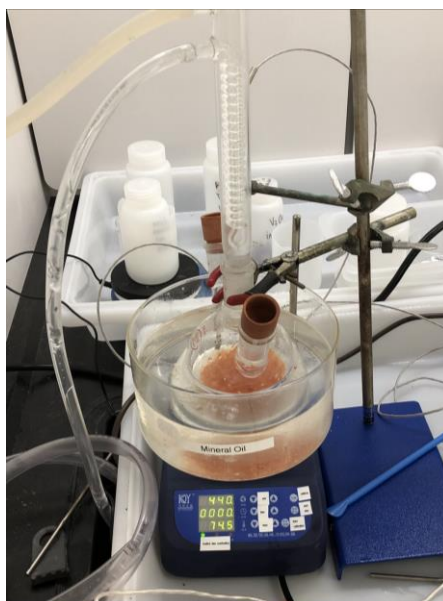


Figure 3.2: The reflux setup for the KOH step of the procedure

These chitosan dominant shells were annealed at 750 °C for 1 hour,² with a ramp rate of 3 °Cmin⁻¹ under Argon in a Sentro Tech vacuum furnace.⁴



Figure 3.3: The vacuum furnace for the carbonization step

The large potassium ions attack the chitosan during the carbonization process, creating a mesoporous structure within the resulting carbon. These potassium ions need to be removed after carbonization so that the mesopores will be left vacant to hold charge. The shells were extensively washed with vacuum filtration and deionized water. Additionally, for this step a centrifuge was used to spin down the shell powder into a pellet so that the supernatant could be disposed. Fresh deionized water was poured back into the centrifuge tube and the tube was vortexed to resuspend the powder in water. These steps were repeated several times to ensure that all the residual potassium ions were removed. The composition of the shells after this step was verified using EDS and pH measurements

to make sure that all potassium ions had been removed. Due to the induced potassium activation during carbonization, the resulting powder was activated carbon.



Figure 3.4: Hitachi S-3400 SEM used for EDS measurements

3.2 Electrode Preparation

The active material is milled for 1 hour in a SPEX Sample-Prep 8000M mill with 5mm diameter Ytria stabilized zirconia balls and ethanol to reduce particle size. The material is then dried and put through a 325-mesh sieve for uniformity. The electrodes are prepared by punching 12mm diameter substrates composed of carbon-coated copper, or aluminum Foil (components from Xiamen Tmax Battery Equipment LTD). The electrode is chosen to have a ratio of 80% crawfish derived activated carbon, which are nitrogen doped for internal and surface structure improvement; 10% polyvinylidene difluoride (PVDF) from MTI Corp. for increased energy density and thermal stability; and 10% carbon black (Alfa Aesar super P, 99%) with high conductivity to improve electrolyte

distribution. These elements are mixed via mortar and pestle and 1ml of N-Methyl-2-pyrrolidinon (99.5% from Acros Organics) is added as a solvent. It is ground into a homogenous slurry and mixed by hand for at least 10 minutes until no individual particles are visible. 50um of the slurry is then deposited onto the foil substrate via micro pipette and placed in a 60C oven overnight to dry. Finally, the electrodes are vacuum annealed at 110°C for 4 hours to remove any residual moisture.



Figure 3.5: The SPEX mill used to prepare the carbonized material

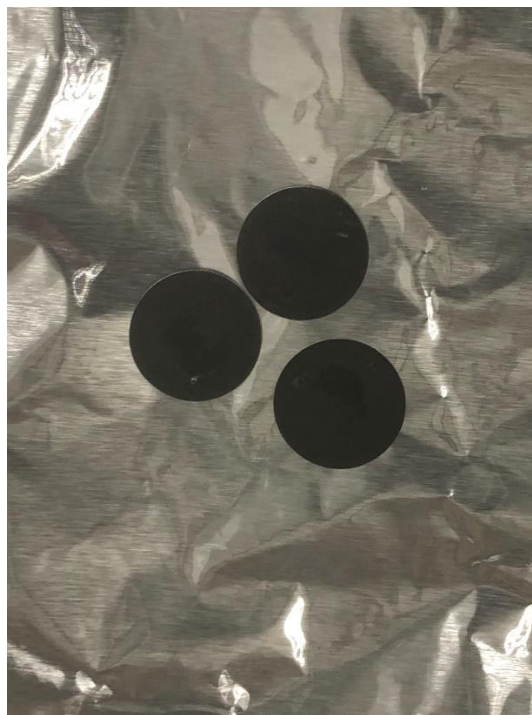


Figure 3.6: Prepared electrodes using Al current collectors and drop casting

3.3 Cell Assembly

CR2032 coin cell batteries (components from Xiamen Tmax Battery Equipment LTD) are assembled in a glovebox under Argon using glass microfiber separators from GE healthcare/Whatman and Sodium from Afla Aesar, 99%. Furthermore, the electrolyte used to saturate the electrode directly depends on the mesoporous structure of the carbon material. Therefore, 1M sodium hexafluorophosphate ethylene carbonate in diethyl carbonate (NaPF_6 EC+DEC) is chosen for the crawfish activated carbon electrode. This aqueous electrolyte provides an increase in ionic conductivity due to its stability and solubility in the solvent, providing consistent performance over many charge and discharge cycles.



Figure 3.7: (From Left to Right) The positive battery lid, an electrode, the glass fiber separator, a piece of raw sodium, the stainless-steel current collector, a washer spring, and the negative terminal of the coin cell. Also pictured is a bottle of the NaFP₆ electrolyte.



Figure 3.8: The cell press used to crimp the coin cells

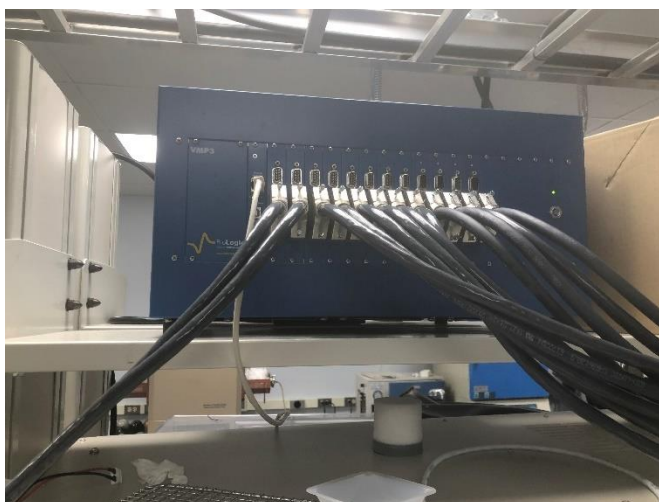


Figure 3.9: An assembled CR2032 coin cell

For electrochemical evaluation, cyclic voltammetry (CV) testing was performed using a Bio-Logic VMP3 and EC-lab software. Long term cycling and anode rate capability was performed using LANHE LAND CT2001A battery testing system and its monitoring software. All cells were tested at 30°C inside a temperature-controlled chamber.



Figure 3.10: The LANHE cyclor channels with connections running to the environmental chamber adjacent



Figurer 3.11: The Biologic VMP3 Potentiostat used for CV measurements



Figure 3.12: The inside of the environmental testing chamber

4. RESULTS

4.1 Shell Biorefinery

There are two phases of outcomes for this procedure, a successful yield of nitrogen-doped activated carbon with a mesoporous structure, and satisfactory performance in electrochemical testing. The former of these can be confirmed by performing EDS (HITACHI S-3400, the 4800 model was used for imaging) to find out material composition, using pH to check for trace elements from previous steps, and by taking high magnification photographs of the treated carbon. From the 30lbs of live crawfish that were boiled, de-shelled, dried overnight, and then blended to a small particle size about 450 g of shell powder was produced. Of that 450g, about 100g was taken and dried for a second time, leaving 87.4g of completely dry shells shown in Figure 4.2. After 24 hours at room temperature in 10% wt. HCl, the dried shells showed in Figure 4.3 weighed only 22.3g. The shells displayed in Figure 4.4 were washed to neutral and put into the heated NaOH solution, and massed only 18.68 g after the soak. Next, they were refluxed in 40% wt. KOH and weighed 12.45g after this step. This powder was placed in the furnace under Ar for 1h at 750 °C with a ramp rate of 3 °Cmin⁻¹ and weighed 3.73 g post-carbonization. That yielded 4.27% wt. of the mass of the dried, untreated shells. EDS results of the sample before-during-and after all of these steps are below. As seen in Figure 4.5, the nitrogen composition is 12.5% wt. before carbonization, greater than the 8.69% wt. in chitosan⁶ which was the goal in the nitrogen-doping process. Notice that post carbonization, the potassium is washed away from 2.86% wt. (Figure 5) to 0.38% wt. (Figure 4.7), as it is no longer needed. A Brunauer-Emmett-Teller (BET) surface analysis machine was used to calculate the BET surface area and micropore volume (using T-plot method). The pre-

measurement annealing was performed at 200C to remove any absorbed water. From figure 4.1, the BET surface area of the crawfish was found to be 312.2 m²/g. The adsorption average pore width (4V/A by BET) was 30.7 Å, with a BJH Desorption average pore width (4V/A) of 19.0Å. Lastly, the average particle size was found to be 195.4Å. A high-magnification image of this surface can be seen in Figure 4.8.

Surface Area	
Single point surface area at P/Po = 0.295112000:	312.1663 m ² /g
BET Surface Area:	307.1300 m ² /g
t-Plot Micropore Area:	308.4914 m ² /g
t-Plot External Surface Area:	-1.3614 m ² /g
BJH Desorption cumulative surface area of pores between 17.000 Å and 3000.000 Å width:	2.1133 m ² /g
Pore Volume	
Single point adsorption total pore volume of pores less than 0.000 Å width at P/Po = 1.000061378:	0.235954 cm ³ /g
t-Plot micropore volume:	0.158048 cm ³ /g
BJH Desorption cumulative volume of pores between 17.000 Å and 3000.000 Å width:	0.001004 cm ³ /g
Pore Size	
Adsorption average pore width (4V/A by BET):	30.7302 Å
BJH Desorption average pore width (4V/A):	19.007 Å
Nanoparticle Size	
Average Particle Size	195.357 Å

Figure 4.1: Results from the BET analysis

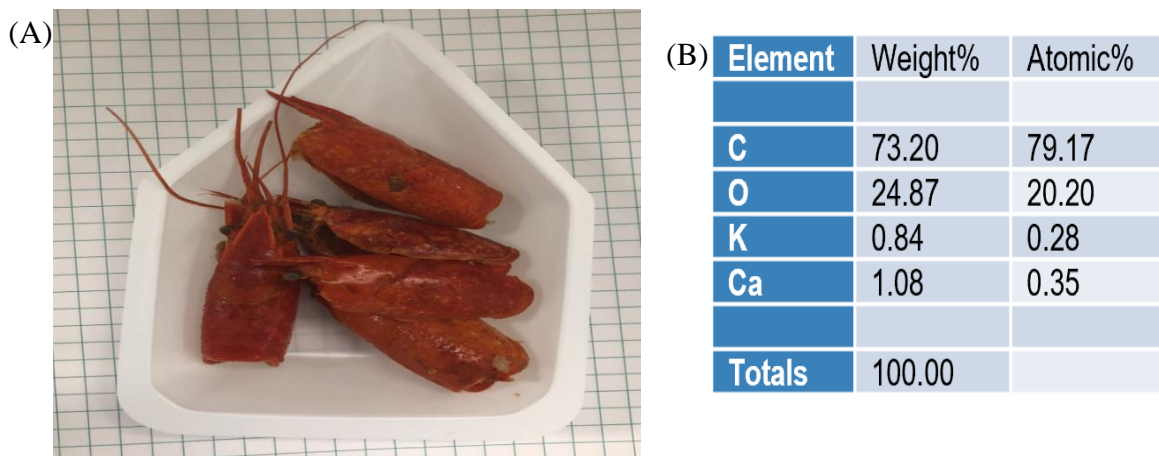


Figure 4.2: (A) Crawfish shells after the boiling and drying process. (B) EDS produced table showing the elemental weight and atomic percents of the boiled crawfish.

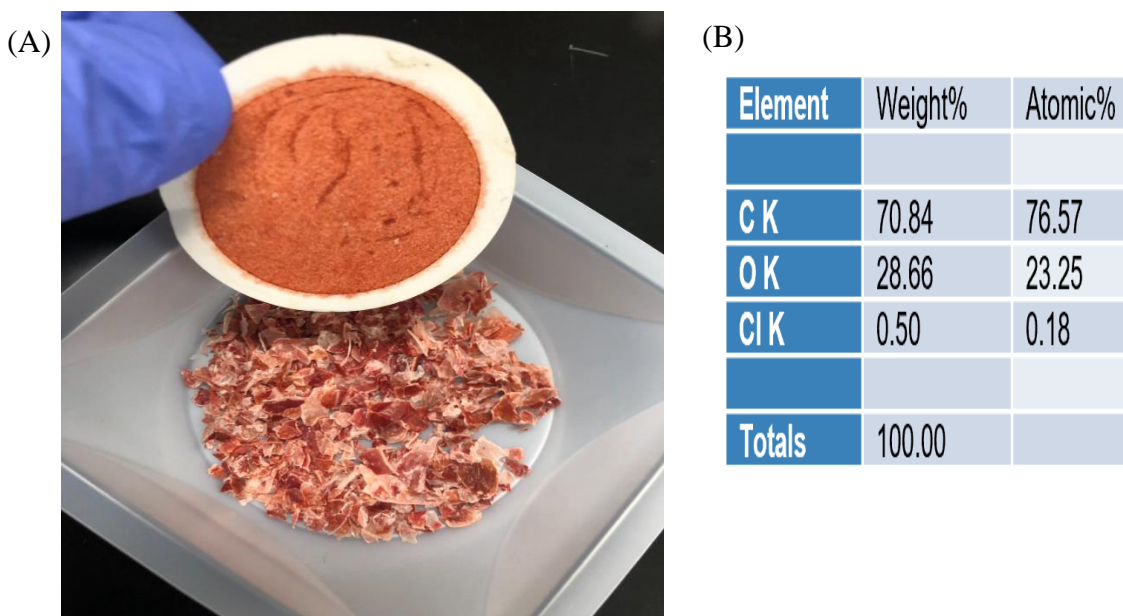


Figure 4.3: (A) Crawfish shells after being soaked in HCl. (B) EDS produced table showing the elemental weight and atomic percents of the HCl soaked crawfish after washing.

(A)



(B)

Element	Weight%	Atomic%
C	54.36	61.41
O	45.24	38.36
Na	0.37	0.22
Cl	0.03	0.01
Totals	100.00	

Figure 4.4: (A) Deproteinized chitin dominant crawfish after being soaked in NaOH. (B) EDS produced table showing the elemental weight and atomic percents of the NaOH soaked crawfish after washing.

(A)



(B)

Element	Weight%	Atomic%
C K	41.94	50.19
N K	11.84	12.15
O K	38.94	34.98
K K	7.25	2.66
Ca K	0.03	0.01
Totals	100.00	

Figure 4.5: (A) Deacetylated chitosan dominant crawfish shells after being refluxed in KOH. (B) EDS produced table showing the elemental weight and atomic percents of the KOH refluxed crawfish.

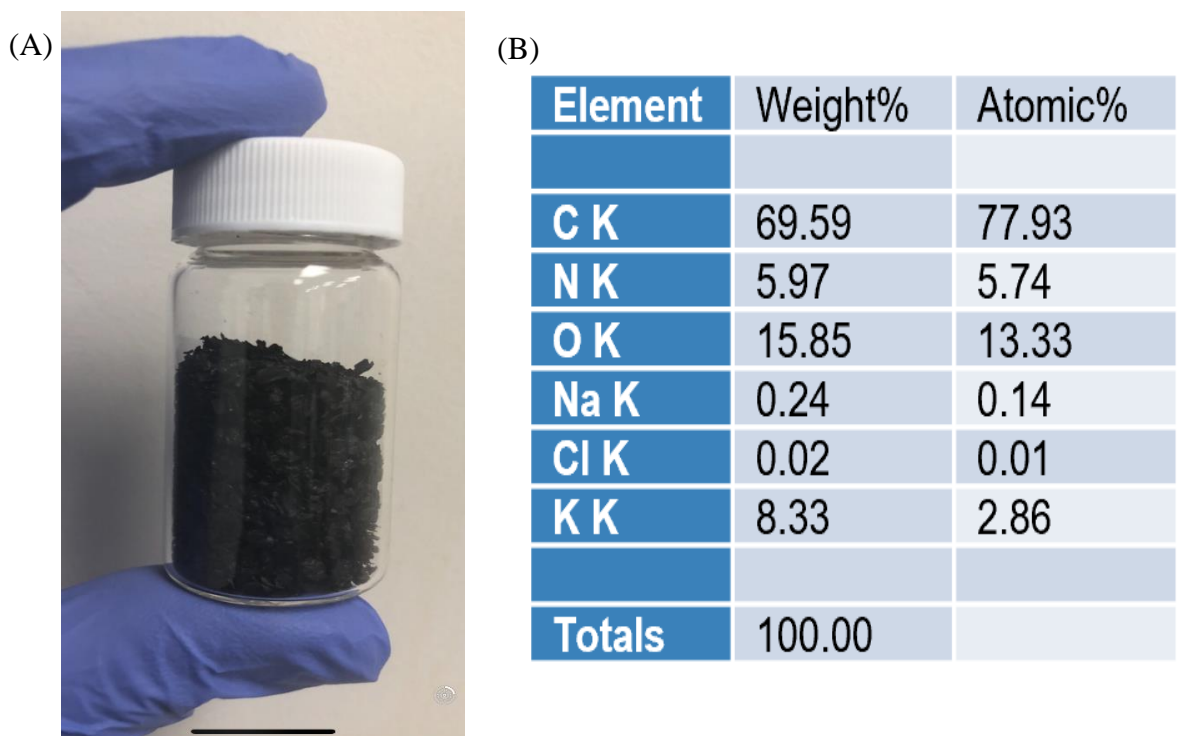


Figure 4.6: (A) Carbonized biomass. (B) EDS produced table showing the elemental weight and atomic percents of the carbonized crawfish.

Element	Weight%	Atomic%
C K	94.95	96.72
O K	3.76	2.87
K K	1.22	0.38
Ca K	0.07	0.02
Totals	100.00	

Figure 4.7: EDS produced table showing the elemental weight and atomic percents of the carbonized and washed crawfish.

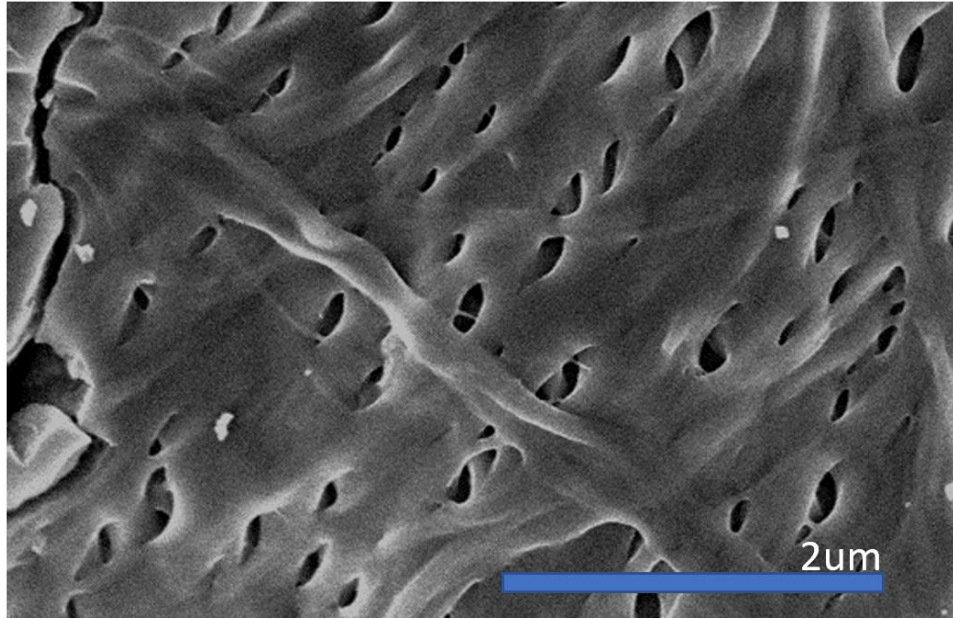


Figure 4.8: High magnification SEM image (HITACHI S-4800) showing the mesoporous structure of the activated carbon.

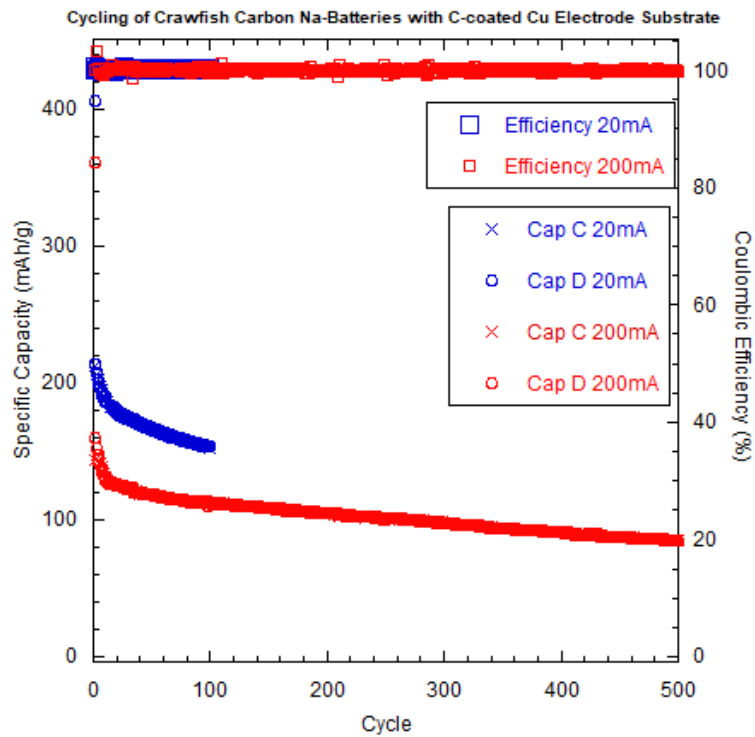


Figure 4.9: Long term cycling at 20mA/g on electrode with active loading of $1.12\text{mg}/\text{cm}^2$ and 200mA/g on electrode with loading of $1.27\text{mg}/\text{cm}^2$

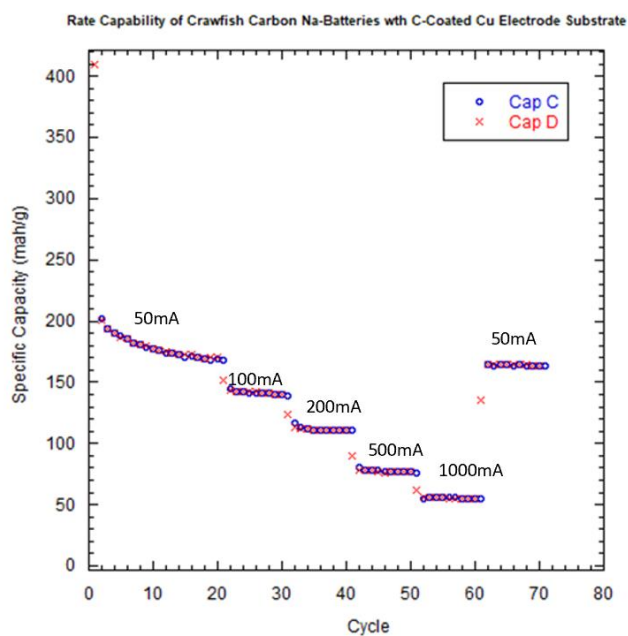


Figure 4.10: Rate Capability performed at 50mA/g, 100mA/g, 200mA/g, 500mA/g, 1000mA/g, and 50mA/g respectively on C-Cu substrate electrode with active mass loading of $1.24\text{mg}/\text{cm}^2$.

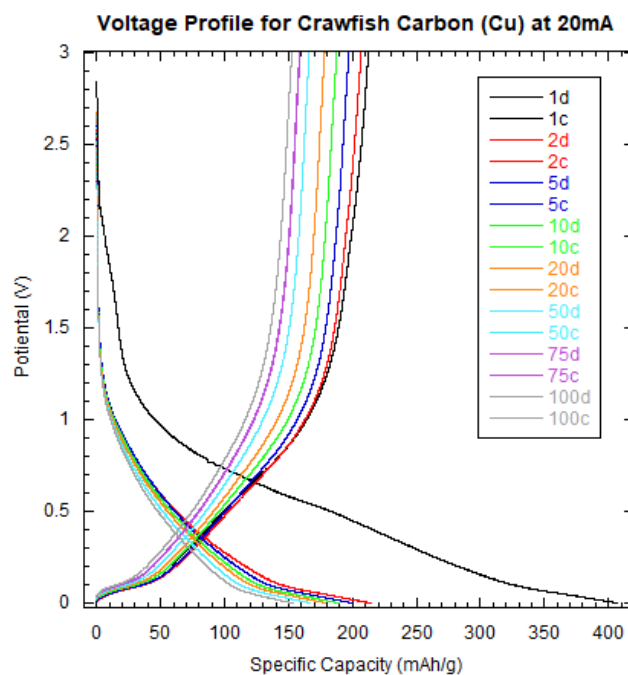


Figure 4.11: Voltage profile of the $1.12\text{mg}/\text{cm}^2$ loaded cell from figure 8 for selected cycles.

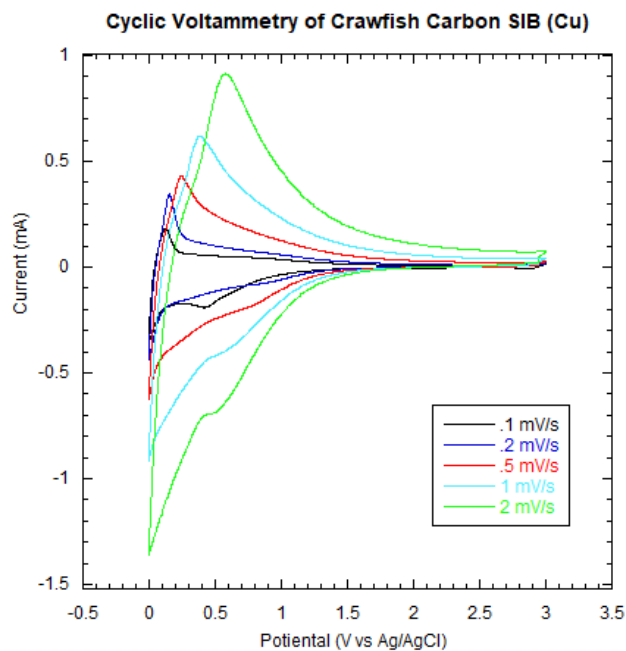


Figure 4.12: CV performed on a cell with loading of $1.15\text{mg}/\text{cm}^2$ on carbon coated copper substrate.

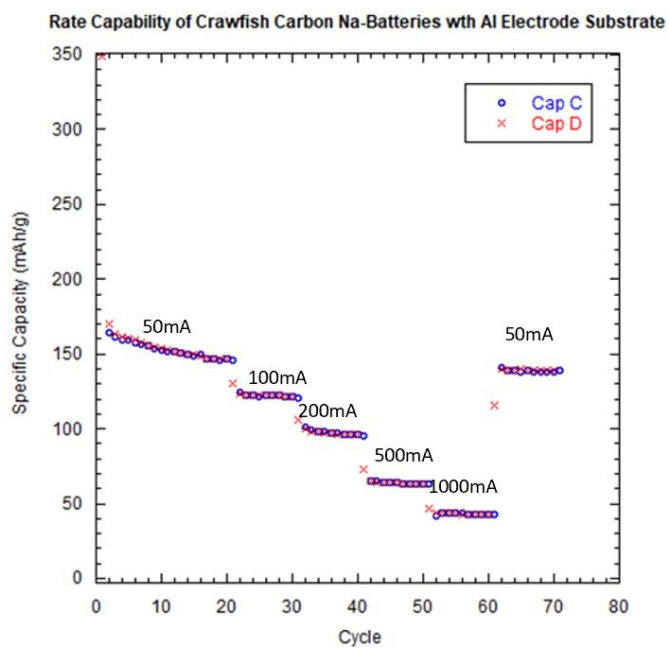


Figure 4.13: Rate capability performed at 50mA/g, 100mA/g, 200mA/g, 500mA/g, 1000mA/g, and 50mA/g respectively on Al substrate electrode with active mass loading of $1.24\text{mg}/\text{cm}^2$

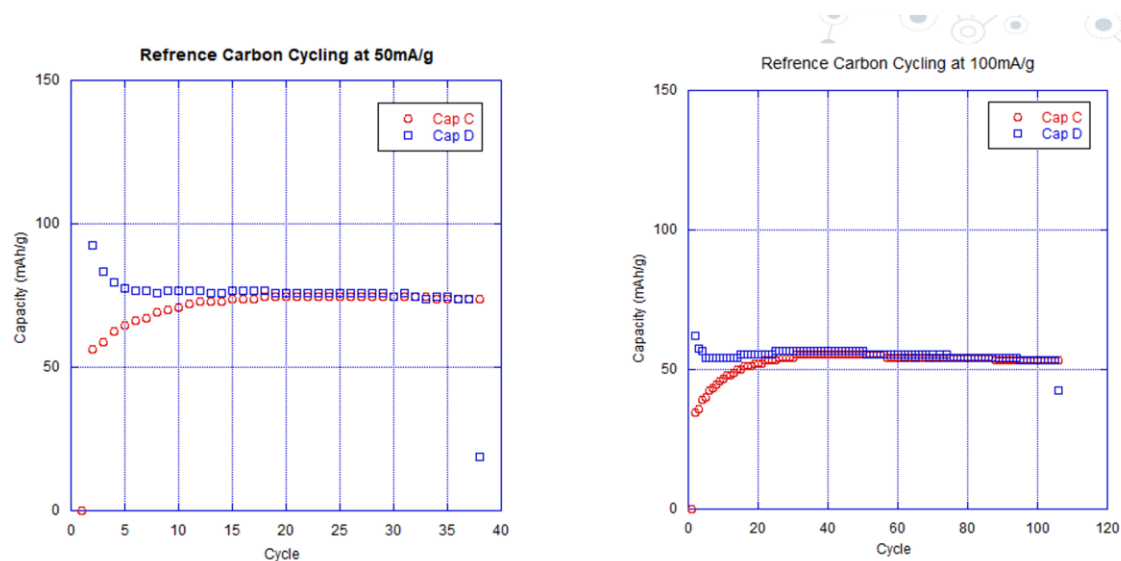


Figure 4.14: Cycling performance of graphite reference cells with loading of $1.19\text{mg}/\text{cm}^2$ at $50\text{mA}/\text{g}$ and $1.02\text{mg}/\text{cm}^2$ at $100\text{mA}/\text{g}$

4.2 Electrochemistry

For electrochemical performance evaluation, we performed long term cycling, anode rate capability, and cyclic voltammetry. As seen in figure 4.9; the material achieved respectable capacity upwards of $175\text{mAh}/\text{g}$ at low rates and above $100\text{mAh}/\text{g}$ for over 300 cycles before performance decreased. This is comparable, if not better than performance on commercially available activated carbon in Na half cells, which has a reported capacity of $\sim 160\text{mAh}/\text{g}$ at low rates of $.1\text{C}$ and under $100\text{mAh}/\text{g}$ at higher rates of 4C .⁷ Notable also is the much higher discharge capacity and greater than 100% efficiency for both cells on the first cycle. This can potentially be attributed to several to sever factors such as the

sodium binding to impurities, formation of a solid electrolyte interface, or general capture by the material due to its mesoporous structure. In figure 4.11 a steady decrease in capacitance is observed as the specific current used to charge the cell is increased from 50mA/g to 1000mA/g. This near 300% decrease in performance is indicative that this carbon material isn't an ideal candidate for high-rate charging. However; it achieves a capacity of 164mAh/g when returned to 50mA/g current. This is almost identical to the last discharge of 169mAh/g after the first 20 cycles. This indicates that the material does have some high resistance to degradation.

From figure 4.12 a large I-R drop is observed for all cycles show. Although the cell does have a high OCV greater than 2.8V, approaching our voltage window ceiling; it quickly drops without gaining any capacity. This is the opposite of ideal battery performance, where minimal I-R drop occurs and the slope of the discharge plot would only be slightly negative and only falling off near maximum capacity. This I-R drop can be attributed to impurities in the material due to its waste-derived nature, non-ideal assembly, or the equivalent series resistance of the cell (comprised of both membrane resistance of charge transport and interfacial resistance with the NaPF₆ electrolyte). From figure 4.12 it can be found that the cell has a high internal resistance, indicated by the narrow shape of the curve.

As mentioned, Al foil was also tested due to its higher availability and lower cost than Cu. Even still, a capacity of 150mAh/g was achieved at low rates of 50mA/g. It exhibited similarly poor performance to the C-Cu system at higher rates. But considering the active material is repropose waste and the cost of Al foil is almost negligible, this is respectable performance. For comparison and validation, reference cells with graphite

(Alfa Aesar, APS 7-11 Micron) were assembled. When compared to the performance reported in figure 4.14; both crawfish systems nearly double this capacity, validating to some degree that this bio-refinery process increases performance to when compared to un-activated carbon.

5. DISCUSSION

This investigation shows that crawfish shell bio-waste can be processed into a novel energy storage material for use as an active material in electrodes for sodium ion batteries. The biorefinery process contains many different applications to improve material properties as to increase the specific capacitance. As reported, the main drawback of amorphous hard carbon is the sluggish kinetics and mediocre conductivity.¹⁸ The processing of the chitin into chitosan to result in nitrogen doped activated mesoporous carbon was performed to mediate these limitations. However, the capacity is still not exceptional, but considering this is a waste product, it is high enough to validate the process.

Procedurally, the shell bio-refinery was extremely successful. This is confirmed by the EDS results that reinforce the reasoning behind the treatments and their predicted effects were achieved experimentally. One non ideality of this process however is the involvement of HCl treatment, as hazardous materials should be avoided if possible and present issues when scaling. Additionally, the high weight loss experienced during the carbonization step is expected, but leaves less usable material than desired. The most encouraging of this though was the successful activation of the carbon while retaining high nitrogen content. However, the surface area achieved was much lower than predicted, so further refinement in this step is likely needed if better performance is desired to match the performance of highly activated mesoporous sheets of doped carbon material.¹⁸ The cycling results are encouraging however as they are higher than that reported in commercially available carbons in Na half cells.⁷ They also used an identical voltage window and Copper foil, be it not Carbon Coated.⁷ The differences in these systems

however, is that the electrolyte used for that research was 1M NaClO₄ while we used NaPF₆. Both were dissolved in 1:1 DEC and EC:DEC. Additionally, their cells were assembled using a 2430-coin cell with a three electrode setup with 2 sodium foils as the other electrodes.⁷

Insight about the electrochemical performance of this cell can be gained by examination of the voltage profile curves. We can see that the I-R drop exhibited is quite substantial and only increases in intensity with time. After the first cycle, more than half of the cell's potential is instantly lost before gaining even 10mAh/g of capacity. This is severely impacting the performance of the cell, and if further development is pursued, should be an area of focus. Additionally, the slope of the successive discharges continues to increase, while having to try and accommodate for this at lower and lower potentials to gather capacity. One way to potentially solve this issue would be to attempt to try and exfoliate the material into nano-sheets while retaining its mesoporous structure. Some work has been done on nitrogen doped mesoporous carbon that has been processed into spheres and shown very promising performance; with specific capacities of 334mAh/g at 50mA/g rates.¹⁸ This is an increase of almost 100% of the performance of the crawfish shells after their initial capacity loss during the first few cycles. Similar to the study mentioned previously, they also used 1M NaClO₄ as their electrolyte.¹⁸ This could be explored as a way to increase performance of the crawfish carbon in half cells, as we were only tested using NaPF₆. However, all of these other systems were using pristine starting material for refinement and testing, which does not align with the original purpose of this investigation.

The only investigation using NaPF₆, Na 2032 half cells, and 8:1:1 ratio of active material: carbon black: PVDF binder in the slurry, got their activated carbon from waste

materials of discarded electronics.²⁰ In this very similar system they were only able to achieve a long-term capacity of <150mAh/g at a current density of 20mA/g. I feel that this is the fairest comparison since it has the most similar parameters. However, their slurry was mechanically stirred for 24h, electrode sheets pressed in a hot plate, cells cycled in an argon environment, and used a voltage window of .1-2.5V. These are all parameters designed to increase the performance of the system, besides arguably the voltage window, and yet the crawfish were still able to out perform this material. Additionally, 20mA/g was the highest current reported, while the crawfish were able to maintain a similar capacity at a rate an order of magnitude higher.²⁰ This is most likely due to the inherent structure of the Chitin, and the nitrogen doping. However, in a very direct comparison, the crawfish are more justified as a starting material considering the relative effort required in processing is similar.

7. CONCLUSION

Activated carbon derived from the biorefinery of crawfish shells with the outlined procedure and testing conditions was found to be a novel electrochemical material which produces respectable energy storage per mass capabilities when compared to that of other commercially available activated carbons. While by definition the carbon has been activated, the resulting surface area is lower than that of other readily available materials such as YP-50.⁸ A nitrogen content of 5.97%wt. after annealing was comparable to the 5.8% wt. achieved by other shell-derived activated carbons,⁴ which was on the higher end of the range reported. To obtain higher nitrogen doping, it is possible that the activation temperature could be increased without a notable effect on the nitrogen saturation. This could help to increase electrical conductivity which is a concern for hard carbon.¹⁹ Energy storage capabilities exceeding other activated carbons and traditional hard carbon validate this method for use, with even higher performance possible if the mesoporous structure can be developed more thoroughly. However, the process is time consuming and better performance is necessary for it to be viable when compared with highly developed energy storage materials.¹⁸

8. REFERENCES

- [1] Chen, X., Yang, H., and Yan, N. (2016) Shell Biorefinery: Dream or Reality?, *Chemistry* 22, 13402-13421.
- [2] Wang, L., Zheng, Y., Wang, X., Chen, S., Xu, F., Zuo, L., Wu, J., Sun, L., Li, Z., Hou, H., and Song, Y. (2014) Nitrogen-Doped Porous Carbon/Co₃O₄ Nanocomposites as Anode Materials for Lithium-Ion Batteries, *ACS Applied Materials & Interfaces* 6, 7117-7125.
- [3] Yang, F., Zhang, Z., Xingxing, K., Wei, Z., Yanqing, C., and Li, L. (2015) Dopamine derived nitrogen-doped carbon sheets as anode materials for high-performance sodium ion batteries, *Carbon* 91, 88-95.
- [4] Gao, F., Qu, J., Zhao, Z., Wang, Z., and Qiu, J. (2016) Nitrogen-doped activated carbon derived from prawn shells for high-performance supercapacitors, *Electrochimica Acta* 190, 1134-1141.
- [5] V. Sattayarut , C. Chanthad , P. Khemthong , S. Kuboon , T. Wanchaem , M. Phonyiem , M. Obata , M. Fujishige , K. Takeuchi , W. Wongwiriyan , P. Khanchaitit and M. Endo. (2019) Preparation and Electrochemical Performance of Nitrogen-enriched Activated Carbon Derived from Silkworm Pupae Waste, *RSC Adv.*, 2019, 9 , 9878.
- [6] Luzardo-Álvarez, A., Antelo-Queijo, A., Soto VH., and Blanco-Méndez, J. (2011) Preparation and Characterization of β -Cyclodextrin-Linked Chitosan Microparticles, *Journal of Applied Polymer Science* 123, 3595–3604.
- [7] Qi Li, Youyu Zhu, Pinyi Zhao, Chao Yuan, Mingming Chen, Chengyang Wang, (2017) Commercial activated carbon as a novel precursor of the amorphous carbon for high-performance sodium-ion batteries anode, *Carbon*, Volume 129, 2018, Pages 85-94, ISSN 0008-6223,
- [8] Yanhong Lu, Suling Zhang, Jiameng Yin, Congcong Bai, Junhao Zhang, Yingxue Li, Yang Yang, Zhen Ge, Miao Zhang, Lei Wei, Maixia Ma, Yanfeng Ma, Yongsheng Chen, (2017) Mesoporous activated carbon materials with ultrahigh mesopore volume and effective specific surface area for high performance supercapacitors, *Carbon*, Volume 124, 2017, Pages 64-71, ISSN 0008-6223,
- [9] Simon, P., Gogotsi, Y., and Dunn, B. (2014) Where Do Batteries End and Supercapacitors Begin?, *Science* 343, 1210.

- [10] Śliwak, A., Díez, N., Miniach, E., and Gryglewicz, G. (2016) Nitrogen-Containing Chitosan-Based Carbon as an Electrode Material for High-Performance Supercapacitors, *Journal of Applied Electrochemistry* 46, 667-677.
- [11] Rinaudo, M. (2006) Chitin and chitosan: Properties and applications, *Progress in Polymer Science* 31, 603-632.
- [12] Zou, B.-X., Wang, Y., Huang, X., and Lu, Y. (2018) Hierarchical N- and O-Doped Porous Carbon Composites for High-Performance Supercapacitors, *Journal of Nanomaterials* 2018, 1-12.
- [13] Zou, B.-X., Wang, Y., Huang, X., and Lu, Y. (2018) Hierarchical N- and O-Doped Porous Carbon Composites for High-Performance Supercapacitors, *Journal of Nanomaterials* 2018, 1-12.
- [14] Björn Bolund, Hans Bernhoff, Mats Leijon, vFlywheel energy and power storage systems, (2004) *Renewable and Sustainable Energy Reviews*, Volume 11, Issue 2, 2007, Pages 235-258, ISSN 1364-0321,
- [15] Manish K. Rathod, Jyotirmay Banerjee, Thermal stability of phase change materials used in latent heat energy storage systems: A review, *Renewable and Sustainable Energy Reviews*, Volume 18, 2013, Pages 246-258, ISSN 1364-0321,
- [16] Ali Eftekhari, Dong-Won Kim, Sodium-ion batteries: New opportunities beyond energy storage by lithium, *Journal of Power Sources*, Volume 395, 2018, Pages 336-348, ISSN 0378-7753,
- [17] Ali Eftekhari, On the Theoretical Capacity/Energy of Lithium Batteries and Their Counterparts, (2019) *ACS Sustainable Chem. Eng.* 7, 4, 3684-3687.
- [18] Xiongwei Zhong, Yinghzi Li, Laiheng Zhang, Jun Tang, Xiangnan Li, Chang Liu, Mengmeng Shao, Zhougang Lu, Hui Pan, Baomin Xu. High Performance Sodium-Ion Batteries Based on Nitrogen-Doped Mesoporous Carbon Spheres with Ultrathin Nanosheets (2018). *ACS Appl. Mater. Interfaces* 2019, 11, 3, 2970–2977
- [19] Kim, D. Y., Kim, D. H., Kim, S. H., Lee, E. K., Park, S. K., Lee, J. W., Yun, Y. S., Choi, S. Y., & Kang, J. (2019). Nano Hard Carbon Anodes for Sodium-Ion Batteries. *Nanomaterials (Basel, Switzerland)*, 9(5), 793. <https://doi.org/10.3390/nano9050793>
- [20] Uttam Kuman, Damian Goonetilleke, Vaibhav Gaikwad, James C. Pramutida, Rakesh K. Joshi, Neeraj Sharma, Veena Sahajwalla. Activated Carbon from E waste Plastics as a Promising Anode for Sodium-Ion Batteries (2019). *ACS Sustainable Chem. Eng.* 10310-10322